

# Experimental Study of Flow-Induced Noise in a Backpack Vacuum Cleaner

## Brandon Foo, Dave Matthews and Jie Pan

Department of Mechanical Engineering, The University of Western Australia, Perth, Australia

#### **ABSTRACT**

Backpack vacuum cleaners are widely used in both domestic and commercial environments. As these machines operate in close proximity to the user's ears, their noise generation and control have become important concerns for acousticians and manufacturers alike. This experimental study demonstrates that flow-induced noise is the dominant contributor to the sound pressure level (dBA) experienced by operators. The rotating blades inside the vacuum chamber interact with the unsteady airflow along the entire flow path, generating both a narrowband blade-passing component and a broadband turbulent component. The former arises from blade-passing forces, while the latter is influenced by the acoustic and vibrational resonances of the chamber. Experimental evidence is presented to support these observations.

## 1 INTRODUCTION

Noise analysis and control in vacuum cleaners remain a global challenge due to their impact on users and the complex aerodynamic, electrical, and structural mechanisms involved. Jeon et al. (2004) identified the dominant noise source as the aerodynamic interaction between the impeller and diffuser; uneven impeller pitch affected sound quality without altering SPL or performance, while a tapered, inclined trailing edge design reduced tonal noise. Mahjoob and Ashrafi (2007) optimized air passage geometry in handheld cleaners for noise reduction.

Jafar et al. (2018) measured overall SPL using a hemispherical microphone array and applied Microflown Scan & Paint to locate sources, also evaluating dust filters as sound-absorbing materials. Teoh et al. (2023) achieved a 7.4 dB(A) reduction in canister cleaners by incorporating polypropylene sound panels and a honeycomb filter. Cudina and Prezelj (2007) provided a systematic overview of suction unit noise, distinguishing airborne from structure-borne contributions. They showed that motor-driven structure-borne noise diminishes with higher flow rates and vaned diffusers, though the latter increase rotational and turbulent noise, raise costs, and reduce flow efficiency.

In this paper, the noise of a backpack vacuum cleaner is investigated experimentally, aiming for a further understanding of the noise generation mechanisms. Noise from the vacuum cleaner is characterized by tonal and broadband components. The properties of those noise components are determined by the angular velocity of the cleaner's rotor unit and the frequency response of impeller cavity. By using a variable voltage transformer, the sound and vibration of the vacuum cleaner at various rotor rpm were examined. Using the torque-voltage relationship of a universal motor, the time-dependent model of the rotor dynamics was developed for describing the starting, steady state and turned-off stages of the rotor angular velocity. This makes it possible to study the nature of blade passing tonal noise and broad band noise for different rotor velocities.

## 2 DESCRIPTION OF EXPERIMENT

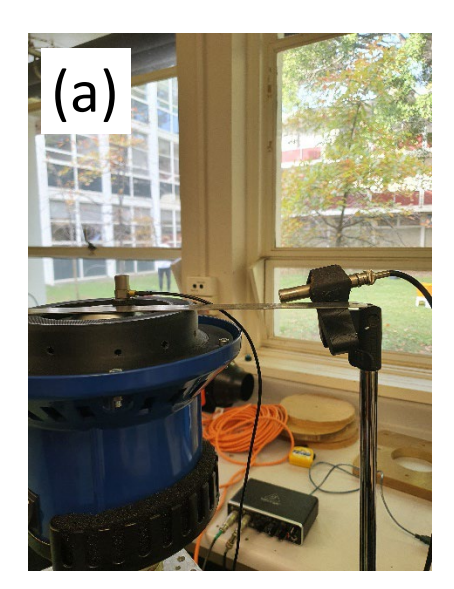
Figure 1(a) shows the set-up for measuring the noise, vibration, forces and flow rate of the vacuum cleaner. For easy assessment of the impeller's rpm, the external plastic casing and air-filter of the cleaner were removed. The noise from the cleaner is measured using a BSWA microphone placed 15cm away from the centre axis of the

ACOUSTICS 2025 Page 1 of 8

impeller and 3cm above the impeller casing. A B&K (B&K2307) accelerometer is attached using a magnet to the top of the impeller casing (see Figure 1(b)) for monitoring the vibration of the cleaner. Mounted on a six-axis force/torque sensor system from ATI Industrial Automation, the aerodynamic reaction forces and torques on the vacuum unit were determined. The rpm of the nine impellers was measured by an optical tachometer (Digitech). The airflow rate at the inlet was measured by an anemometer from Benetech (GM8903). The vacuum cleaner is driven by a universal motor. A variable electric transformer from Powertech (SRV-5) was connected between the 240V main power supply and the electrical input of the motor so that the response of the cleaner can be examined at various speed.

Both microphone and accelerometers were calibrated. Their outputs were fed into a two-channel external sound card (Behringer UMC202HD) with an adjustable gain and then converted to digital signals by Audacity (with sampling frequency at 44100Hz) for further analysis. Samples of sound and vibration are processed by Matlab.

The measurement of the vacuum cleaner was conducted in a large laboratory environment with adequate sound absorption from side walls. The vacuum cleaner is mounted on a solid support and 1 m from the floor surface. The background noise and vibration were checked. The signal to noise ratio is above 10 dB.



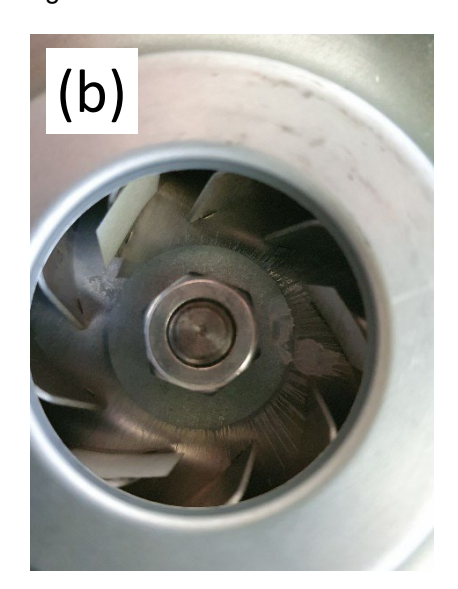


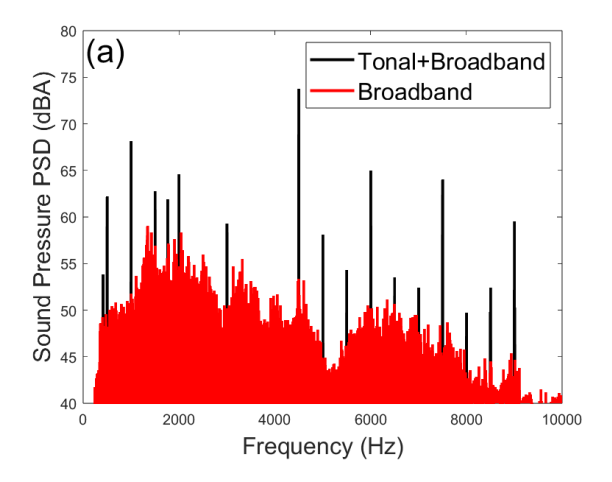
Figure 1: (a) microphone and accelerometer for the experimental study of the vacuum cleaner, (b) impellers, impeller casing and air-inlet.

## 3 RESULTS AND DISCUSSION

Figure 2(a) presents the A-weighted power spectral density (PSD) of vacuum cleaner noise at 240 V, with an overall level of 83 dBA. Blade-passing components occur at 4502 Hz (74 dBA) and 9006 Hz (60 dBA), while additional tonal components from motor excitation appear at 500 Hz, 1 kHz, and harmonics. The strongest motor-induced tone at 1 kHz is 6 dB below the first blade-passing component. With tonal contributions removed (see the red curve in Figure 2(a)), the broadband noise level is 82 dBA, indicating broadband noise dominance, though tonal components, particularly at blade-passing frequencies, remain perceptually significant.

Since the sound radiation from the vacuum cleaner can also be through structure-borne paths, the PSD of the acceleration at the impeller casing is also measured and shown in Figure 2(b).

Page 2 of 8 ACOUSTICS 2025



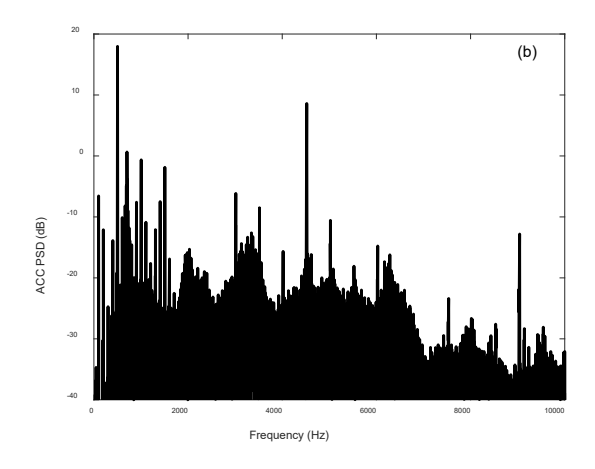


Figure 2: PSD of (a) sound pressure and (b) acceleration of the vacuum cleaner for 240V electrical input

#### 3.1 Rotor dynamics

Both blade passing noise and broad band noise is dependent on the rpm of the rotor (including the rotor of the electric motor and the impeller unit). The rpm (angular velocity) of the rotor can be determined by the rotor dynamics and nature of the torque generated by the electric motor used for the vacuum cleaner. Universal motors are commonly used for vacuum cleaners, as they could reach high angular velocity (20,000–35,000 rpm) which is ideal for generating strong suction. Based on the principle of the interaction force of an electric current in a magnetic field generated by the current, the torque, T, applied on the rotor in the motor is proportional to the square of the current. Therefore, the angular velocity of the rotor,  $\Omega$ , can described as:

$$I\dot{\Omega} + \eta(t)\Omega = T(t) \tag{1}$$

where I is the mass moment of inertial of the rotor. The angular velocity of the rotor can be readily solved if a step torque is applied to the rotor, corresponding to the switching-on and off processes of the voltage input to the vacuum cleaner:

$$T(t) = \begin{cases} T_0 & 0 \le t \le t_0 \\ 0 & 0 \ge t \ge t_0 \end{cases}$$
 (2)

where  $t_0$  is the duration of the cleaner being turned on and  $T_0$  is the torque applied by the motor, which is approximately proportional to the voltage squared.  $\eta$  is the damping constant which could be different between switching on and off processes of the motor:

$$\eta(t) = \begin{cases} \eta_{on} & 0 \le t \le t_0 \\ \eta_{off} & 0 \ge t \ge t_0 \end{cases}$$
(3)

The damping appears larger during the switching-on process because of the induced electric current in the closed-loop of the motor. The electrical damping is not present at the switching-off process for the open-circuited motor. Assuming the initial condition of the rotor as  $\Omega_0 = 0$ , the angular velocity of the rotor is solved as:

$$\Omega(t) = \begin{cases}
\frac{T_0}{\eta_{on}} (1 - e^{-\frac{\eta_{on}}{I}t}), & 0 \le t \le t_0 \\
\frac{T_0}{\eta_{on}} (1 - e^{-\frac{\eta_{on}}{I}t_0}) e^{-\frac{\eta_{off}}{I}(t - t_0)}, & t \ge t_0
\end{cases}$$
(4)

ACOUSTICS 2025 Page 3 of 8

The expression of the step response in Equation (4) is used to explain the spectrograms of the noise and vibration of the vacuum cleaner as shown in Figure 3.

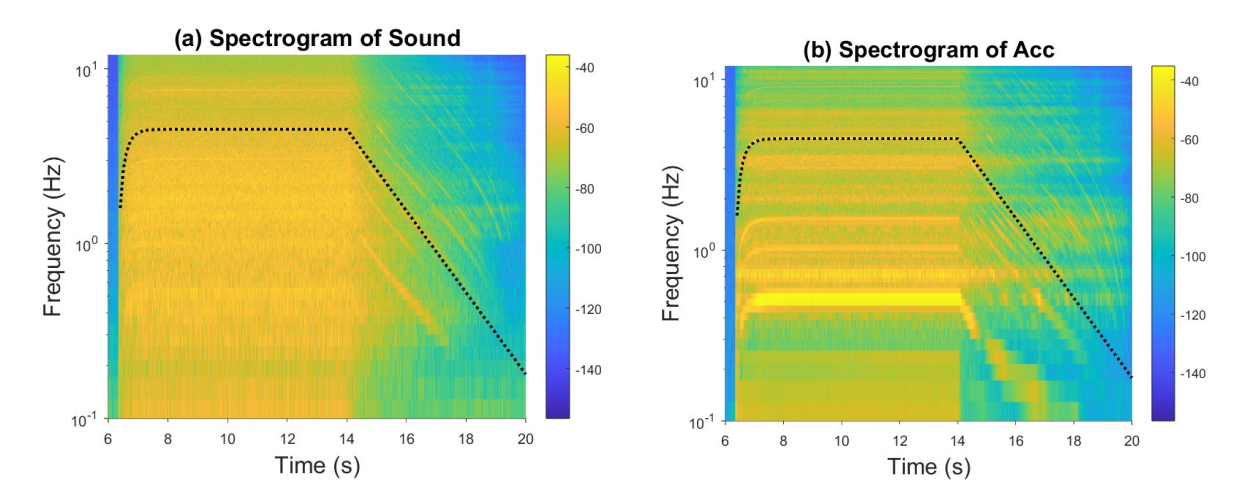


Figure 3: Spectrograms of the sound pressure (a) and casing acceleration (b) of the vacuum cleaner for applied voltage at 240V. The cleaner was switched on at t=6.3s and of at t=14s. The dotted curves are the predicted BPF using Equation (4)

In Figure 3, families of step response are observable in both spectrograms of the sound and vibration. The most distinguished step responses belong to the family of blade passing tonal noise and vibration at 4502 Hz and 9006 Hz. They are caused by the periodically impulsive (with period of whole rotation of the rotor) aero-dynamic force between the nine impellers and fast changing flow velocity field close to the impellers. Other families of step response are more observable in the spectrogram of the casing vibration. The mechanisms of those families are not clear. However, they are characterized by the harmonics of 50Hz and 100Hz, indicating that they are probably related to the electrical-magnetic forces.

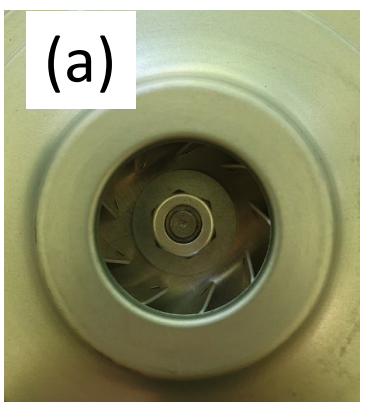
The decay curves of the angular velocity in the spectrograms of the noise and vibration are not exactly linear in the logarithmic scale. This indicates that the linear damping model in Equation (1) could only serve as an approximation. The energy loss in the rotor dynamics is not only caused by the friction in the bearings, but also by the aerodynamic and electro-magnetic interactions.

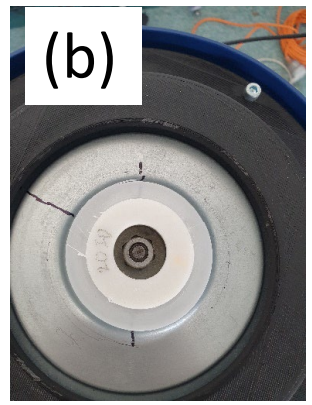
The blade passing frequency observed in Figure 3 can be simulated using Equation (3) via extracting parameters  $\frac{T_0}{\eta}$ ,  $\frac{\eta}{I_o}$  and  $t_0$ . Using the step response for the 1st BPF in Figure 3, those parameters are obtained as  $\frac{T_0}{\eta} = 4502 \mathrm{Hz}$ ,  $\frac{\eta_{on}}{I} = 4.368 \mathrm{s}^{-1}$ ,  $\frac{\eta_{off}}{I} = 0.5376 \mathrm{s}^{-1}$  and  $t_0 = 7.7 \mathrm{s}$ . The step responses of the first blade passing frequency of the sound and vibration are presented in Figure 3 by the dotted curves.

#### 3.2 Effect of input Voltage on the noise and vibration

To examine the noise and vibration characteristics of the vacuum machine as a function of input voltage, three inlet configurations were tested. The "original" configuration, shown in Figure 4(a), consists of an untreated inlet with a diameter of 32 mm. The "annulus" configuration (Figure 4(b)) has a reduced inlet diameter of 20 mm. The "custom" configuration (Figure 4(c)) has the same inlet cross-sectional area, featuring a central hole with a diameter of 14 mm and 18 uniformly distributed oval openings. Each oval has a major radius of 2.09 mm and a minor radius of 1.09 mm.

Page 4 of 8 ACOUSTICS 2025





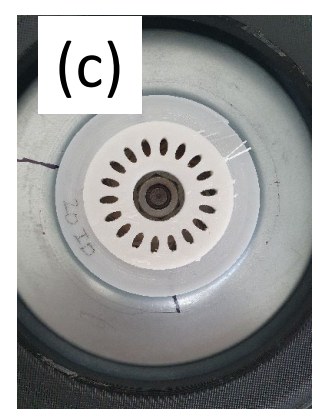


Figure 4: Three inlet configurations for examining the noise and vibration from the vacuum cleaner (a) Original, (b) Annulus, and (c) Custom

The angular velocity of the rotor—and therefore the blade-passing frequencies of the sound and vibration—is a function of the input voltage. The first two blade-passing (BP) frequencies for the three configurations are shown in Figure 5 as functions of input voltage.

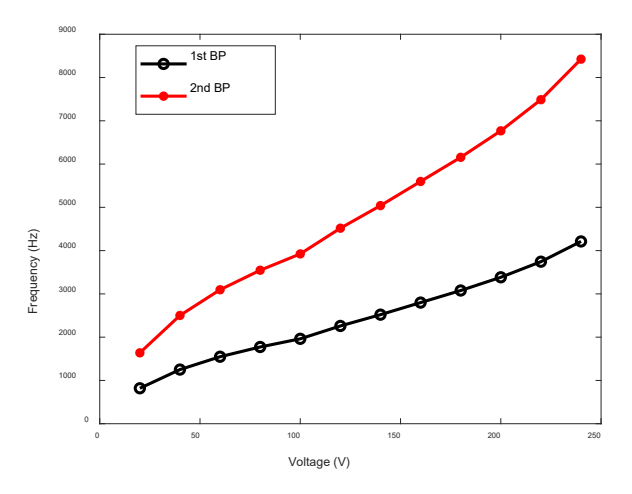


Figure 5: First two blade passing frequencies (BPFs) of the vacuum machine as a function of input voltage

Figure 6 presents the sound pressure power spectral density (PSD) of the vacuum machine at the first two blade-passing frequencies. In general, the sound pressure level at these frequencies increases with input voltage, which can be attributed to the enhanced interaction between the blades and airflow as the rotor angular velocity increases. However, the noise level at each blade-passing frequency is also influenced by the frequency response of the air cavity formed by the impeller casing and by the sound radiation characteristics of the casing structure. These factors may explain why the sound pressure PSD does not increase linearly with input voltage.

The inlet configurations not only exhibit different cavity frequency response characteristics but also affect the blade–airflow interaction at the inlet. Due to the combined influence of these two effects, the impact of configuration on the sound pressure PSD at the blade-passing frequencies becomes dependent on both frequency and input voltage. It is also noteworthy that, at the operating voltage of 240 V, the sound pressure PSD at the blade-passing frequencies remains approximately the same for all three configurations.

ACOUSTICS 2025 Page 5 of 8

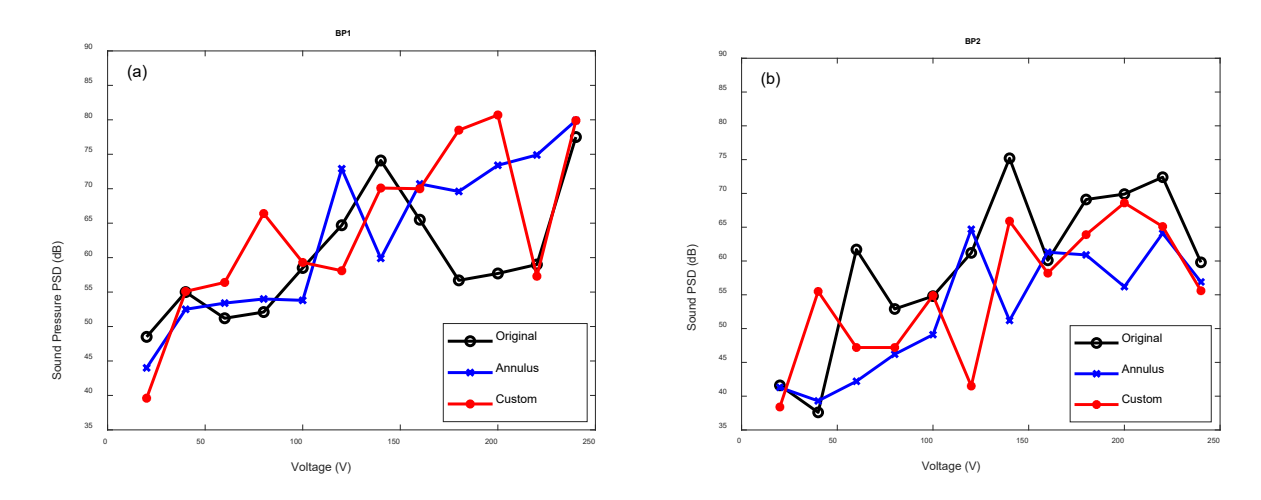


Figure 6: Sound pressure PSD at (a) first blade passing frequency, (b) second blade passing frequency

The acceleration PSD of the casing structure is presented in Figure 7. It can be seen that reducing the inlet opening area in the annulus and custom configurations decreases the vibration and noise levels at the second blade-passing frequency (see Figure 7(b) and Figure 6(b)) when the input voltage is greater than 100 V. However, a clear increase in casing vibration is observed at the first blade-passing frequency for both the annulus and custom configurations.

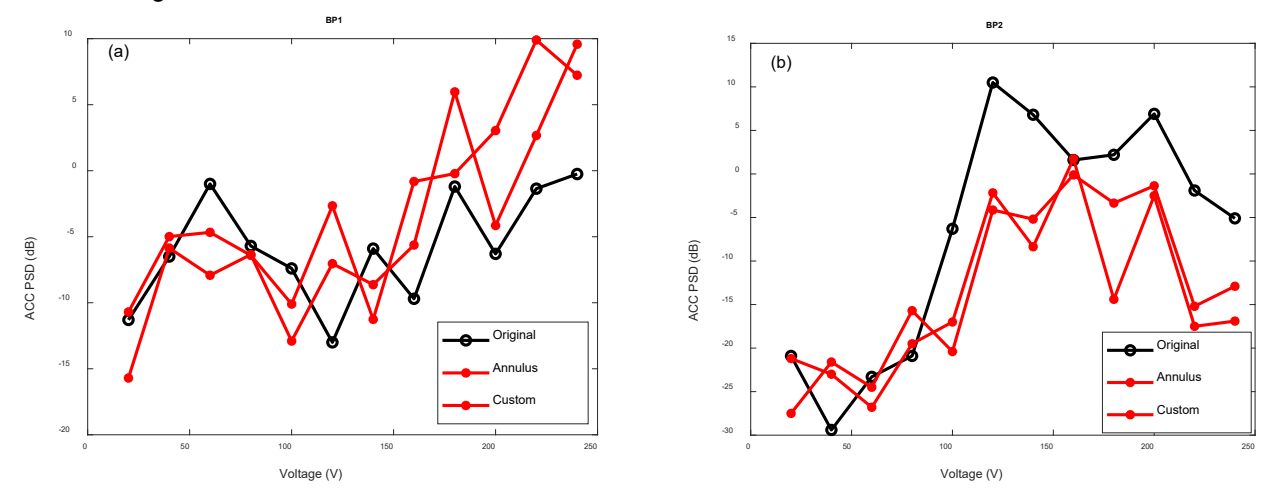
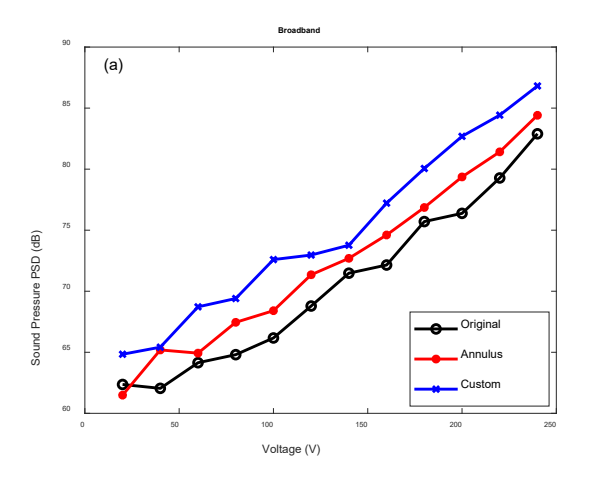


Figure 7: Acceleration PSD of the casing structure at (a) first blade passing frequency, (b) second blade passing frequency

The broadband sound pressure PSD and acceleration PSD for the three configurations are compared in Figure 8. Reducing the cross-sectional area at the inlet clearly increases the broadband noise and vibration levels of the vacuum machine. The noise level from the Custom configuration is approximately 5 dB higher than that of the Original configuration, while the Annulus configuration shows an average increase of about 2 dB compared with the Original configuration.

Page 6 of 8 ACOUSTICS 2025



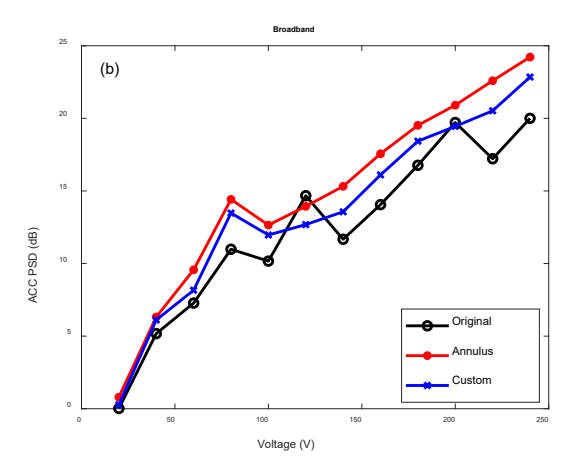


Figure 8: Broadband sound pressure PSD (a) and broadband acceleration PSD (b) for three inlet configurations of the vacuum cleaner

#### 4 CONCLUSIONS

The noise and vibration of a backpack vacuum cleaner were experimentally examined as functions of input voltage. Variations in the blade-passing noise frequencies, induced by periodic flow-impeller interactions, are directly linked to changes in the rotor system's angular velocity, which are accurately predicted by a rotor dynamics model. The vacuum cleaner noise consists of two major components. The tonal component arises from blade-passing interactions and electromagnetic forces of the motor, while the broadband component mainly originates from turbulent airflow within the cleaner's air path. Both components are radiated through the air and structural paths. The broadband noise power spectral density (PSD) exceeds the tonal PSD by approximately 8 dB, indicating that turbulence noise reduction is critical for overall noise control. Although having lower PSD, the blade-passing and electrical noises remain clearly audible due to their tonal and persistent characteristics. The effect of inlet geometry was investigated using annulus and custom configurations to simulate reductions in cross-sectional area. An increase in airflow velocity into the vacuum chamber led to higher broadband noise levels. The custom configuration produced higher sound levels than the annulus configuration, suggesting that the distributed small oval openings further increased local flow velocity and turbulence noise. The significant variation of blade-passing noise with input voltage reflects the combined influence of cavity and casing resonances on the radiated tonal noise, as well as the impact of inlet flow restriction on impeller-flow interaction and the amplitude of the bladepassing noise. The vibration of the casing structure of the vacuum cleaner is also measured and shows nonnegligible contribution to tonal and broadband noise.

#### **REFERENCES**

Jeon, W. H., H. S. Rew and C. J. Kim, 2004. Aeroacoustic Characteristics and Noise Reduction of a Centrifugal Fan for a Vacuum Cleaner, KSME International Journal, Vol. 18(2), 185-192.

Mahjoob, M.J. and H. Ashrafi, 2007. Noise reduction of handheld vacuum cleaners according to geometric optimization of air passages, ICSV14, Cairns • Australia, 9-12.

Jafar, N. A., W. Ali, and L. E. Ooi, 2018, Noise reduction using flax and kenaf for household vacuum cleaner, Journal of Engineering Science and Technology Vol. 13(11), 3566 – 3576.

Teoh, C. Y., J. Lim, M. N. A.Hamid, L. E. Ooi, and W. H. Tan, 2023. Suppression of Flow-Induced Noise of a Canister Vacuum Cleaner, International Journal of Integrated Engineering, Vol. 15(1), 180-190.

Cudina, M. and Jurij Prezelj, 2007. Noise generation by vacuum cleaner suction units. Part I. Noise generating mechanisms – An overview, Applied Acoustics 68, 491–502.

ACOUSTICS 2025 Page 7 of 8

Proceedings of ACOUSTICS 2025 12-14 November 2025, Joondalup, Australia

Cudina, M. and Jurij Prezelj, 2007. Noise generation by vacuum cleaner suction units. Part II. Effect of vaned diffuser on noise characteristics, Applied Acoustics 68, 503–520.

Cudina, M. and Jurij Prezelj, 2007. Noise generation by vacuum cleaner suction units. Part III. Contribution of structure-borne noise to total sound pressure level, Applied Acoustics 68 521–537.

Page 8 of 8 ACOUSTICS 2025